8th CIRP Conference on Intelligent Computation in Manufacturing Engineering

# Condition monitoring of an ultra high pressure intensifier for water jet cutting machines

M. Goletti[a,*], M. Grasso[a], M. Annoni[b], B.M. Colosimo

*aLaboratorio MUSP, Via Tirotti, 9, I-29122 Piacenza, Italy*
*bDipartimento di Meccanica, Politecnico di Milano, via La Masa, 1, I-20156 Milano, Italy*
* Corresponding author. Tel.: +39-(0)523-623190 ; fax: +39-(0)523-645268  *E-mail address:* massimo.goletti@musp.it

**Abstract**

The most important advantages of water jet are the capability to cut nearly every material, the low cutting temperature and the negligible cutting forces. When end users are interviewed, most of them point out that the most critical problem of water jet machines is the reliability of the system components, together with the difficulty in estimating their life time. As far as the UHP (Ultra High Pressure) intensifier is concerned, there are several components that work under extreme fatigue conditions, as the pressure inside the cylinders can reach 400 or even 600 MPa. Nearly every critical component is located into the UHP intensifier, but different failure scenarios can be envisaged, leading to different pattern deviations from nominal behavior conditions. In this paper a correlation analysis on multiple signal features with the health status of the machine is presented. Then a multi-sensor based monitoring approach is discussed and tested on a real case study: it is based on the usage of control charts for in-control region definition and possible detection of faults.

© 2013 The Authors. Published by Elsevier B.V.
Selection and peer review under responsibility of Professor Roberto Teti

*Keywords:* Waterjet; Condition Based Maintenance; Statistical Process Control; multi-sensor monitoring.

## 1. Introduction

The reliability of water jet cutting machines is a topic of main concern in the industrial field as various problems may arise during the process: machine stops due to faults, leakages, damages to the workpiece, etc. Corrective maintenance is the widest exploited strategy with pour results in terms of productivity. As in many other fields, the best way to optimize the performances of a machine tool is to introduce CBM (Condition Based Maintenance) strategies, but their management is quite challenging and reliable condition monitoring systems are required. There is a great number of works concerning water jet machine monitoring ([1] to [5]), mainly based on acoustic emission (AE) sensors. The goals of these works are different, from nozzle wear monitoring to remote controlled applications in inaccessible environments.

In this paper, the attention is focused on the working condition of the CMS Tecnocut 60 HP pump intensifying machine. This machine is able to reach more than 400 MPa by means of 3 single-acting cylinders with a maximum water flow rate of 5 l/min (orifices up to 0.4 mm in diameter). The condition monitoring must be based on a series of sensors that permits to monitor the working condition of the machine.

In Section 2 the linear position sensors used for condition monitoring are presented. Section 3 describes the real case study used to test the monitoring approach; Section 4 discusses the proposed fault detection and classification methods. Section 5 reports the achieved results and Section 6 eventually concludes the paper.

## 2. Condition monitoring with linear position sensors

There is a wide literature on condition monitoring of waterjet machines with different aims: remote control of

machines [1], control of depth of penetration [2], etc. Many works are based on acoustic emission sensors ([1] to [4]) that are used, for instance in [4], to monitor and to activate a compensation procedure to control nozzle wear by means of an artificial neural network that elaborates frequency domain acoustic signals. In another work [5] the electric input signals is related with mechanical and fluid dynamic signals to design a monitoring system.

In the present paper, a novel approach based on linear position transducers (Gefran ONP1-A) is proposed. The aim of the work is to identify different types of faults that can affect different components of the intensifying pump. The selected transducer is a contactless magnetostative linear position sensor with sliding magnetic cursor and a full scale from 0 to 200 mm. An example of the active stroke of cylinder 2 is reported below.
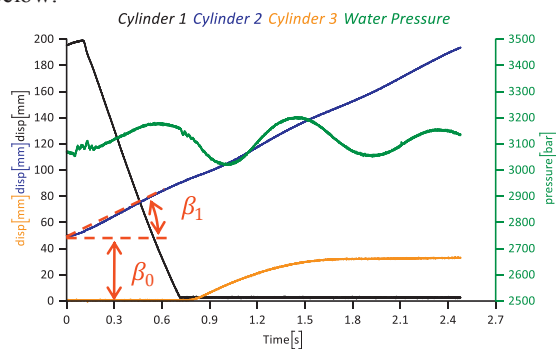


Fig. 1. Compression stroke position for cylinder 2

The first cylinder performs the back stroke in the Fig. 1. When it reaches the end, the third cylinder starts its pre-compression stroke.

A cylinder comprises a certain number of components that are subject to wear or cracks. During the normal machine operations, the pattern of the pre-compression or compression strokes change and a suitable approach can be used to identify it.

The aim of the multi-sensor monitoring approach here described is to classify the behaviour of the pressure intensifier either as normal (i.e. in control) or not by using the multiple linear position signals coming from sensors mounted on pump cylinders. Once the symptom of a fault is detected, the monitoring system should be able to provide information about the fault nature, to properly drive the necessary immediate recovery actions (when required) or the maintenance operations.

## 3. A real case study

A real case study is presented in this section. The selected pump is a 45 kW (model Tecnocut JP 60 HP) intensifying machine with a nominal working point of 413.7 MPa and 5 l/min water flow rate. The cylinder stroke is about 200 mm.

A total of four sensors are used: 3 linear position transducers (described above) and a high water pressure transducer (Gefran TPHA-N-D-V-BO5M). This type of transducer is based on the extensimetric measurement principle with strain gauge on stainless steel. The measuring range is 0 to 500 MPa.

The three position sensors are installed in the back panel of the intensifying pump and the slides are bolted to the stems (see Fig. 2). The water high pressure transducer is mounted on the main line downstream the three cylinders.

The pressure transducer is used in this study to verify the operative conditions during data acquisition tests, performed at the same pressure level, but it is not used for monitoring tasks.
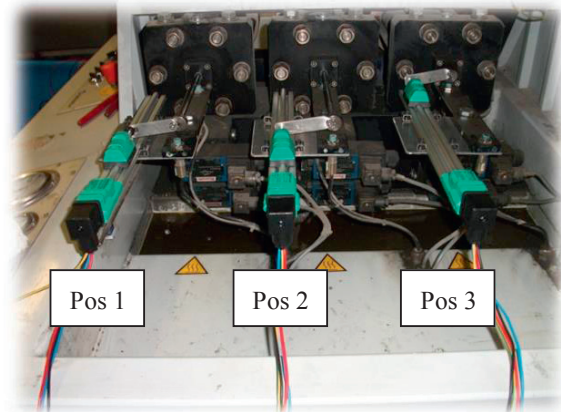


Fig. 2. Experimental setup for the linear position transducer

In this study a set of faulty components were selected by means of an end-user survey on the major problems of AWJ intensifiers. The resulting components are the following: cylinder body, outlet valve body, outlet valve housing and orifice.

A series of screening tests was performed to identify the minimum set of indicators able to detect a fault on the aforementioned components. As it will be seen later, this set comprises two indicators that can be calculated from the sample reported in Fig. 1:

1. The pre-compression stroke $\beta_0$
2. The compression slope (stem speed) $\beta_1$

Both indicators can be computed by a linear regression of the position of the cylinder that is in the compression (active) stroke.

The case study is represented by a full factorial experiment in which new components were compared with cracked and worn ones.

Thus, eventually, four different types of faults are considered, and, for each of them, different samples of

data were collected in randomized order. The considered faults are:

Fault A: Cracked cylinder

Fault B: Cracked delivery valve body

Fault C: Extremely worn delivery valve housing

Fault D: Brocken orifice

Two orifice diameters have been considered: 0.25 and 0.33 mm.

A simple part-program is used in the tests for the production of a 75 mm square plate with four 6.5 mm holes at a nominal working pressure of 350 MPa.

A total of 18 tests replicated 2 times were conducted on 3 days: a total number of 12 replicates under normal conditions and 6 replicates for each fault were performed in order to gather data characterizing both *in-control* and *out-of-control* conditions.

## 4. Fault Detection and Classification

The goal of the condition monitoring system is to detect a possible deviation from the in-control behaviour of the pressure intensifier and to identify which type of fault is the root cause for the out-of-control observations.

It is important to recognize which cylinder is affected by the contingency and to classify the nature of the contingency itself. Furthermore, it is of great importance to distinguish a fault of a pressure intensifier component from any other problems of different nature, with particular regard to possible orifice breakages, that are quite frequent events in waterjet cutting. Such a fault can be easily detected if an operator is supervising the process, but in case of unsupervised operative conditions there is the need to suddenly detect the breakage and stop the process. Thus, the monitoring system should be able to properly classify any out-of-control observation as a symptom of either an orifice breakage or a pressure intensifier fault, to allow the required recovery action.

In order to accomplish such a task it is here proposed to apply a control chart to each couple of synthetic indicators $\boldsymbol{\beta}_i(t) = [\beta_{0,i}(t), \beta_{1,i}(t)]$ associated to $i^{th}$ cylinder ($i = 1,...,N$) at time t, where $N$ is the number of cylinders.

A T$^2$ control chart is used: being $[\boldsymbol{\beta}_i(t_1), \boldsymbol{\beta}_i(t_2),...,\boldsymbol{\beta}_i(t_M)]$ a set of indicator values collected under in-control conditions (i.e. Phase I data), with mean $\overline{\boldsymbol{\beta}}_i = [\overline{\beta}_{0,i}, \overline{\beta}_{1,i}]$ and Variance-Covariance matrix S, the T2 Hotelling's statistics is defined as follows [6]:

$$T_i^2 = \left(\beta_i - \overline{\beta}_i\right)' S^{-1} \left(\beta_i - \overline{\beta}_i\right) \qquad (1)$$

Parameters $\overline{\boldsymbol{\beta}}_i$ and $\boldsymbol{S}$ computed in Phase I are then used to monitor any following observation (Phase II).

When the chart is applied to single observations under the assumption of multi-normality of indicators vectors, the following control limits are typically used [7]:

$$UCL_I = \frac{(M-1)^2}{M} \beta_\alpha\left(\frac{p}{2}, \frac{M-p-1}{2}\right) \qquad (2)$$

$$UCL_{II} = \frac{p(M+1)(M-1)}{M(M-p)} F_\alpha(p, M-p) \qquad (3)$$

Where p is the number of monitored variables (here $p = 2$), and $M$ is the number of observations in Phase I, whereas $\beta_\alpha(\cdot,\cdot)$ and $F_\alpha(\cdot,\cdot)$ are respectively the *100(1-α)* percentiles of Beta and Fisher distributions, with degrees of freedom indicated into brackets.

However, it has been observed in the frame of the study that the selected indicators are typically characterized by a skewed distribution, which violated the multi-normality assumption (e.g., see Fig. 3, where the normal probability plot of indicators $\beta_0$ and $\beta_1$ computed for the real case study described in Section 3 shows a non normal distribution).
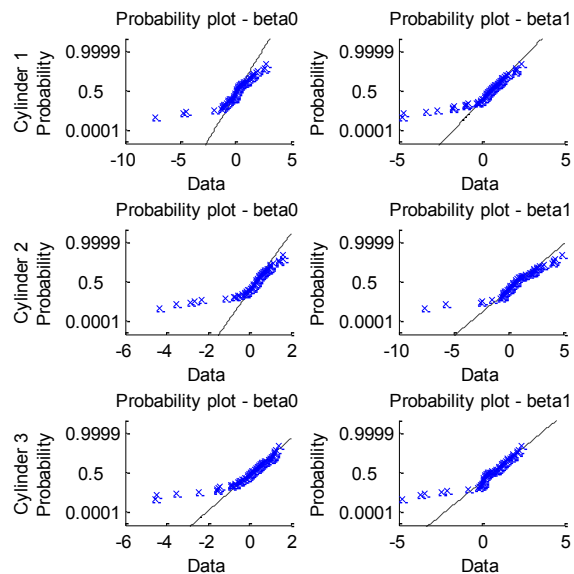


Fig. 3. Normal probability plots for $\beta_0$ and $\beta_1$

This is a frequently encountered situation in practice and different authors have discussed available solutions to face such an issue: Chang and Bai [8] propose a heuristic method to build the chart when data are characterized by skewed distributions, based on an adjustment of covariance matrix; Chen, Kruger et al. [9] present a non-parametric approach based on Kernel

Density Estimation, whereas in [6] the application of the bootstrapping technique for $T^2$ control charts is discussed and compared with other methods; eventually the book of Mason and Young [10] is dedicated to the properties of $T^2$ control charts and deals with the problem of multi-normality violations.

The bootstrap approach is used in this study, accordingly to [6]; it is a widely used resampling with replacement technique which allows determining statistics estimates when the population distribution is not known, and it does not require any data modeling step [11].

The bootstrap-based $T^2$ control charting methods thus works as follows: $T^2$ statistics are computed for each $j^{th}$ bootstrap sample ($j = 1, ... B$) in phase I and the corresponding $100(1-\alpha)$ percentile value is computed; then, the average of B percentiles is used as empirical control limit for the $T^2$ statistics. Here B = 1000 is used.

N control charts must be used at the same time on N different cylinders, and hence the Bonferroni approach is applied to type I error selection, such that $\alpha = \alpha_{fam}/N$, where $\alpha_{fam}$ is the family type I error (here $\alpha_{fam} = 0.0027$ is used).

The usage of a dedicated control chart for each cylinder allows to detect any anomalous behaviour and to rapidly identify the cylinder affected by the contingency. Moreover, when an orifice breakage occurs, all the N control charts are expected to suddenly signal an out-of-control behaviour, and hence a fault involving a single cylinder can be easily distinguished from this latter event.

Further parameters to be used for diagnostic task are the distances $\Delta\beta_{0,i}(t)$ and $\Delta\beta_{1,i}(t)$ defined as follows:

$$\Delta\beta_{0,i}(t) = \left|\beta_{0,i}(t) - \overline{\beta}_{0,i}\right| \qquad (4)$$

$$\Delta\beta_{1,i}(t) = \left|\beta_{1,i}(t) - \overline{\beta}_{1,i}\right| \qquad (5)$$

They are the norm of projections of a vector connecting the Phase I mean $\overline{\boldsymbol{\beta}}_i = [\overline{\beta}_{0,i}, \overline{\beta}_{1,i}]$ with any new observation $< \beta_{0,i}(t), \beta_{1,i}(t) >$ at time t, in the two dimensional feature space spanned by indicators $< \beta_{0,i}, \beta_{1,i} >$.

A crack or an advanced wear level of a valve is expected to cause a large deviation $\Delta\beta_{0,i}(t)$ of indicator $\beta_0$, and a reduced deviation (or possibly no deviation at all) on indicator $\beta_1$: the outlet valve is opened during the compression stroke so it has no influence on the stem speed whilst the pre-compression phase needs the outlet valve to be closed. As a result, cracks or advanced wear cause leakages that change the condition inside the cylinder causing a modification in the pre-compression stroke pattern.

A crack on a cylinder, instead, is expected to cause a deviation for both the indicators as the leakages are present in both pre-compression and compression phases. If a huge crack is present, the pump fails to perform its cycles and the NC goes to duty error.

An orifice breakage, instead, is expected to cause a deviation $\Delta\beta_{1,i}(t)$ of indicator $\beta_1$, and no deviation (or a moderate one) of indicator $\beta_0$ as the orifice define the pump load. Pump load can be seen from the cylinders only in the compression phase. The effect of a broken orifice is expected to be an increment in the diameter so an increment in the required water flow rate (i.e. pump load) and this is expected to be seen in all the three cylinders indicators.

Therefore the bootstrap-based control charts can be coupled with the logging of parameters $\Delta\beta_{0,i}(t)$ and $\Delta\beta_{1,i}(t)$: after any out-of-control detection provided by the charts, the operator can use those deviation parameters to assess which is the most likely root cause of observed symptoms, and hence exploit such additional information to drive the maintenance operations, when required.

Notice that the condition monitoring system here proposed allows both failure detection and classification capabilities by exploiting only the knowledge of nominal (in-control) behaviour of the pressure intensifier, without any need to collect data under faulty conditions, that is always a very complex task.

## 5. Summary of Results

Phase I data were collected under in-control conditions by performing 12 replicates of the same cutting process, described in Section 3. The in-control conditions depend on the selected mean pressure level and orifice diameter (water flow rate), i.e. the pump load. An overall number of M = 100 complete cycles for each cylinder were acquired: first 50 cycles are used as Phase I data, whereas remaining 50 cycles are used to test the chart under nominal conditions.

The indicators vector were standardized by using the sample mean $\overline{\boldsymbol{\beta}}_i = [\overline{\beta}_{0,i}, \overline{\beta}_{1,i}]$ and sample Variance-Covariance matrix S.

Two examples of $T^2$ control charts are reported in Fig. 4 and Fig. 5, where both bootstrap-based and traditional control limits are shown; the former shows the chart referred to cylinder 1 when Phase II is actually in-control, whereas the latter shows the chart for the same cylinder when Fault A (cracked cylinder) is observed.
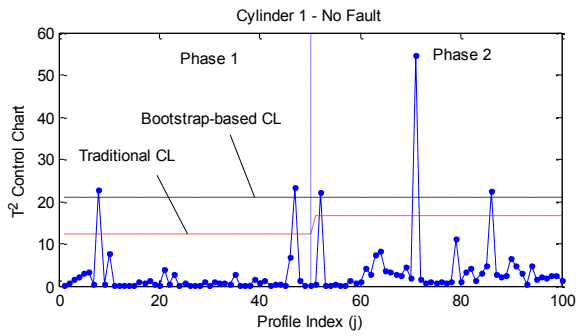
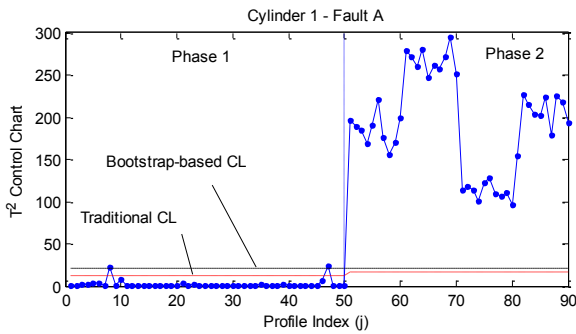Fig. 4. $T^2$ control chart for an in-control process



Fig. 5. $T^2$ control chart for a Fault A in cylinder 1

Fig. 6 shows the percentage of alarms signaled by the control charts in presence of the four different types of fault here considered (percentages are reported for each cylinder).
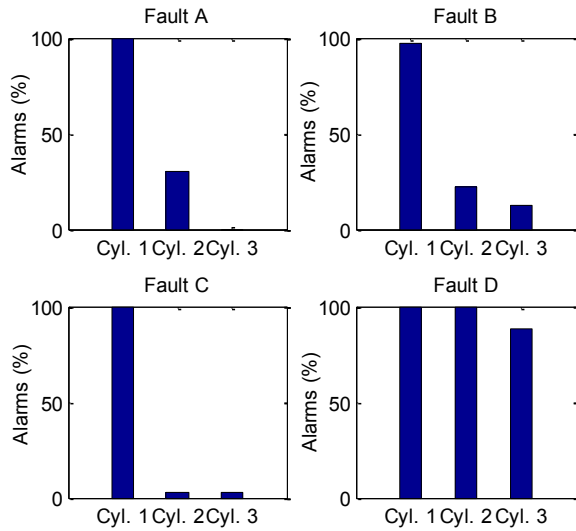


Fig. 6. Percentage of alarms for each considered fault

The figure shows that when Fault A, B and C are injected, the charts properly signal alarms on the cylinder where the fault is present (in this case it is always cylinder #1). Notice that some alarms are

signaled also on next cylinders, but this is physically correct. In fact if a crack or a worn valve is present in $i^{th}$ cylinder, the other two have different operating condition as water pressure is not guaranteed during the cylinder compression stroke, and hence other cylinders cycle is affected by the fault too, even though with a reduced effect.

In presence of fault D (orifice breakage), instead, a high percentage of alarms is signaled on every cylinder, and this is consistent with the nature of the fault.

The inspection of alarms provided by the N control charts allows one to draw preliminary conclusions about the nature of the contingency and its location within the pressure intensifier.

As discussed in the previous Section, further parameters $\Delta\beta_{0,i}(t)$ and $\Delta\beta_{1,i}(t)$ may provide additional information about the root cause of observed alarms.

Fig. 7 reports the boxplots of parameters $\Delta\beta_{0,i}(t)$ and $\Delta\beta_{1,i}(t)$ for the four considered types of fault, computed for the cylinders with higher percentage of alarms, i.e. cylinder 1 for faults A, B, and C, and cylinders 1, 2, and 3 for fault D. The largest difference between mean values $\overline{\Delta\beta_{0,i}(t)}$ and $\overline{\Delta\beta_{1,i}(t)}$ are observed in presence of fault B, C and D, with very low values of $\overline{\Delta\beta_{0,i}(t)}$ with fault B and C, and a very low value of $\overline{\Delta\beta_{1,i}(t)}$ with fault D, in complete accordance with the expected behaviour discussed in previous Section. This means that when a fault involving a valve is present, the most affected indicator is $\beta_0$ (i.e. the excursion in pre-compression phase); when a breakage of the orifice occurs the most affected indicator is instead $\beta_1$ (i.e. the compression speed); and, eventually, when fault A is present both the indicators are affected.

However, the Figure also shows a very large variability of parameters $\Delta\beta_{0,i}(t)$ and $\Delta\beta_{1,i}(t)$, which can be an issue to be faced with if one wants to apply an hypothesis test or a univariate control chart to single indicators, especially when diagnostic conclusions must be drawn from reduced amount of observed data.

The scatter plot shown in Fig. 8 shows how the different types of faults here discussed tend to occupy different portions of the 2D space spanned by indicators $< \beta_{0,i}, \beta_{1,i} >$, with respect to the in-control region, even though the position and dispersion of the clusters of faulty data are expected to vary considerably depending on fault severity (e.g. wear level, dimension of the crack, etc.). Such a variability leads to the need to adopt fault detection and classification methods that exploit only in-control data, as the one here proposed.

## 6. Conclusions

The selected indicators (compression speed $\beta_1$ and pre-compression stroke $\beta_0$) are used to design 3 control charts to monitor the working condition. Each of the

control chart refers to a cylinder, so the fault is directly related to corresponding cylinder.
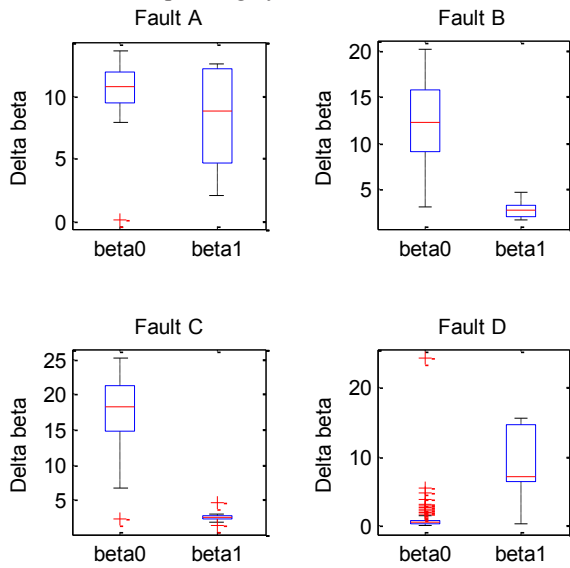


Fig. 7. Boxplots of parameters $\Delta\beta_{0,i}(t)$ and $\Delta\beta_{1,i}(t)$
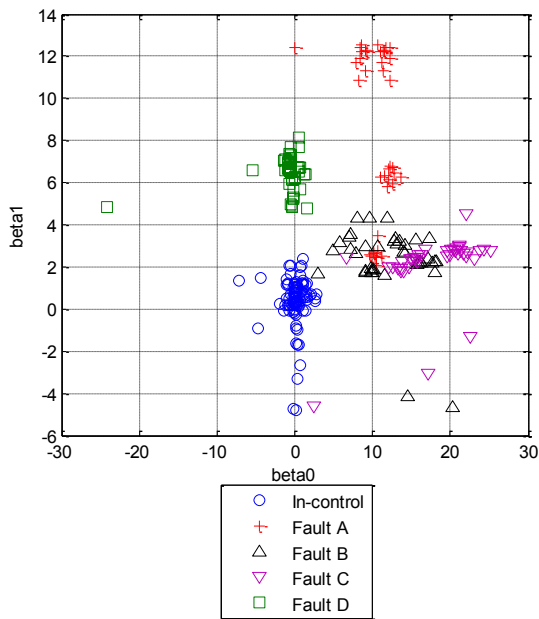


Fig. 8. Scatter plot of the indicators

Selected features allow to properly classify a contingency as a component fault or an orifice breakage. Moreover, the fault detection and classification capability are provided without any need to train the system on faulty data, but only on data acquired under normal behaviour. Another interesting result is that analyzing $\Delta\beta_{0,i}(t)$ and $\Delta\beta_{1,i}(t)$ it is possible to distinguish, inside the cylinder in out-of-control state, among three

faulted components: cylinder body, outlet valve body or outlet valve housing. The system here presented is currently under development in a real-time suite exploitable in industrial environment. However, next steps of the study will be focused on improving the fault classification performances and reducing the false alarm risk.

## Acknowledgements

## References

[1] Louis, H., Meier, G., 1991. "Methods of Process Control for Abrasive Water Jets," 6th American Water Jet Conference, August 24-27, 1991, Houston, Texas, p. 427.

[2] Mohan, R., Momber, A., Kovacevic, R., 1994. On-line Monitoring of depth of AWJ penetration using acoustic emission Technique, Department of Mechanical Engineering and Center for Robotics and Manufacturing System University of Kentucky, 1994, Lexington Kentucky – 40506, USA, p.649.

[3] Axinte, D.A., Kong, M.C., 2009. An integrated monitoring method to supervise waterjet machining. CIRP Annals – Manufacturing Technology, Vol. 58, Issue 1, 2009, University of Nottingham, UK, p. 303.

[4] Mohan, R.S., 1994. Real-time monitoring of AWJ nozzle wear using artificial neural network. Transactions of the North American Manufacturing Research Institute of SME 1994. Vol. XXII. Evanston, IL; USA; 25-27 May 1994 (May 25, 1994), p. 253.

[5] Annoni, M., Cristaldi, L., Lazzaroni, M., 2008. Measurements, Analysis, and Interpretation of the Signals From a High-Pressure Waterjet Pump. IEEE transactions on Instrumentation and Measurement, Vol. 57, no. 1, January 2008 p. 34.

[6] Phaladiganon, P., Kim, S.B., Chen, V.C.P., et al., 2011. Bootstrap-Based T2 Multivariate Control Charts, Communications in Statistics – Simulation and Computation, Vol. 40, Issue 5, pp. 645.

[7] Montgomery, D.C., 2008. "*Introduction to statistical quality control*," John Wiley & Sons, Ed. 6, April 2008.

[8] Chang, Y.S., Bai, D.S., 2004. A Multivariate T2 Control Chart for Skewed Populations Using Weighted Standard Deviations, Quality and Reliability Engineering International, Vol. 30, p. 31.

[9] Chen, Q.,Kruger, U., Meronk, M., Leung, A.Y.T., 2004. Synthesis of $T^2$ and Q statistics for process monitoring, Control Engineering Practise, Vol. 12, p. 745.

[10] Mason, R.L., Young, J.C., 2002. Multivariate Statistical Process Control with Industrial Applications, ASA-SIAM Series on statistics and applied probability.

[11] Hinkley, D.V., 2008. Bootstrap Methods and Their Applications, Cambridge Series in Statistical and Proabilistic Mathematics, Cambridge University Press, 2008.